Structural transformations in amorphous ↔ crystalline phase change of Ga-Sb alloys

T. G. Edwards,[1] I. Hung,[2] Z. Gan,[2] B. Kalkan,[3] S. Raoux,[4] and S. Sen[1]
[1]*Department of Chemical Engineering and Materials Science, University of California, Davis, California 95616, USA*
[2]*Center of Interdisciplinary Magnetic Resonance, National High Magnetic Field Laboratory, 1800 East Paul Dirac Drive, Tallahassee, Florida 32310, USA*
[3]*Advanced Light Source, Lawrence Berkeley Laboratory, Berkeley, California 20015, USA*
[4]*IBM T. J. Watson Research Center, Yorktown Heights, New York 10598, USA*

(Received 19 September 2013; accepted 9 December 2013; published online 20 December 2013)

Ga-Sb alloys with compositions ranging between ~12 and 50 at. % Ga are promising materials for phase change random access memory applications. The short-range structures of two such alloys with compositions $Ga_{14}Sb_{86}$ and $Ga_{46}Sb_{54}$ are investigated, in their amorphous and crystalline states, using ^{71}Ga and ^{121}Sb nuclear magnetic resonance spectroscopy and synchrotron x-ray diffraction. The Ga and Sb atoms are fourfold coordinated in the as-deposited amorphous $Ga_{46}Sb_{54}$ with nearly 40% of the constituent atoms being involved in Ga-Ga and Sb-Sb homopolar bonding. This necessitates extensive bond switching and elimination of homopolar bonds during crystallization. On the other hand, Ga and Sb atoms are all threefold coordinated in the as-deposited amorphous $Ga_{14}Sb_{86}$. Crystallization of this material involves phase separation of GaSb domains in Sb matrix and a concomitant increase in the Ga coordination number from 3 to 4. Results from crystallization kinetics experiments suggest that the melt-quenching results in the elimination of structural "defects" such as the homopolar bonds and threefold coordinated Ga atoms in the amorphous phases of these alloys, thereby rendering them structurally more similar to the corresponding crystalline states compared to the as-deposited amorphous phases.
 [http://dx.doi.org/10.1063/1.4854575]

I. INTRODUCTION

The development of nonvolatile memories with ultrafast read/write speed, based on amorphous ↔ crystalline transformation in phase-change materials (PCMs) is of enormous technological interest.[1,2] PCMs utilize pronounced contrast in optical and/or electrical properties between amorphous and crystalline phases to store binary information. First demonstrated by Ovshinsky in Te-As-Si-Ge system, thin film chalcogenides in the binary systems Ge-Te, Sb-Te and ternary systems Ge-Sb-Te and Ga-Sb-Te, have already been applied to optical recording (DVD-RW, Blu Ray, etc.) and phase-change random access memory (PCRAM).[1–5] Switching in these materials is accomplished through precise thermal cycling, for which heating can transpire via laser irradiation or Joule heating. Crystallization of the amorphous phase occurs when the material is heated above the crystallization temperature, whereas re-amorphization results from a rapid laser heating and melt quenching cycle.

Recently, it has been shown that reducing the Te content of Ga-Te-Sb alloys leads to enhanced performance of PCMs, creating renewed interest in Ga-Sb alloys with Ga contents ranging between ~15 and 50 at. %.[6–11] These binary alloys exhibit marked electrical/optical contrast, ultrafast phase transformation kinetics (few tens of nanoseconds) between the crystalline and amorphous phase, as well as high thermal stability with crystallization temperatures above 200 °C.[8,9,11] The ultrafast timescale of phase switching has been conventionally considered as an indicator of practically diffusionless, displacive transformation and therefore suggests strong structural similarities between the amorphous and crystalline phases. On the other hand, the large change in optical reflectivity or electronic conductivity between the two phases is indicative of significant underlying differences in their electronic structures. However, the atomic scale mechanism of the phase change process in Ga-Sb system is poorly understood, primarily due to the fact that the structures of the amorphous Ga-Sb alloys have remained controversial and largely unexplored, to date. The only known compound in the Ga-Sb system is GaSb, a narrow band gap III-V semiconductor that has been extensively studied for electronic and optoelectronic applications due to its unique physical properties.[12,13] GaSb crystallizes in the cubic zinc blende (ZnS) structure consisting of tetrahedrally coordinated Ga and Sb atoms forming heteropolar Ga-Sb bonds. The structure of amorphous GaSb has been investigated in previous studies using extended x-ray-absorption fine-structure (EXAFS) spectroscopy, x-ray, and neutron diffraction techniques.[14–17] These studies generally concluded that the amorphous state of GaSb could be characterized as a distorted tetrahedral zinc blende structure. Ga K-edge EXAFS spectroscopic results reported a Ga-Sb coordination number of 3.7 in amorphous GaSb and conjectured the presence of possible Ga-Ga homopolar bonds and consequently a violation of chemical order.[14,15] However, the presence of such Ga-Ga bonds would automatically imply the formation of an equivalent fraction of Sb-Sb bonds, provided both Ga and Sb remained tetrahedrally coordinated in the amorphous structure. Although the Sb K-edge EXAFS results

indicated the absence of any significant deviation from tetrahedral coordination for Sb, no evidence of Sb-Sb bonding was found.[15] It may be noted that the presence of chemical order in crystalline GaSb and its violation in the amorphous phase imply that the phase change process would have to be reconstructive in nature, involving bond breaking and atomic rearrangement. The kinetics of such a reconstructive transformation would be slower than that of a purely displacive transformation. On the other hand, for Sb-rich Ga-Sb alloys such as $Ga_{15}Sb_{85}$, crystallization is expected to form a mixture of GaSb and Sb.[9,11,18,19] Crystalline Sb is characterized by a rhombohedral structure with layers of threefold coordinated Sb atoms forming Sb-Sb_3 pyramids. For a purely displacive phase transformation, the structure of the amorphous phase would have to contain amorphous GaSb like domains with tetrahedrally coordinated Ga and Sb atoms, embedded in amorphous Sb where Sb atoms are threefold coordinated. Therefore, it is clear that the application of additional element-specific spectroscopic techniques is needed to address these issues related to the structures of the amorphous Ga-Sb alloys in order to enable the development of a self-consistent structural model of the phase change process. Here, we present the results of a comprehensive, multinuclear (^{71}Ga and ^{121}Sb) NMR spectroscopic study of Ga-Sb alloys, in their amorphous and thermally crystallized states, to directly address the nature of the structural changes associated with the phase change process. We also present synchrotron x-ray diffraction data obtained on the amorphous phases of these alloys that provide complementary evidence supporting the structural conclusions drawn on the basis of the NMR results.

II. EXPERIMENTAL DETAILS

Amorphous films of Ga-Sb alloys with 300 nm thickness and with nominal Ga concentrations of 15 and 50 at. % were deposited on 6 in. diameter Si wafers coated with a 1 μm thick layer of PMMA (poly-methyl methacrylate) using DC magnetron sputtering. For the 50 at. % Ga film deposition was performed using a nominally stoichiometric GaSb target and for the 15 at. % Ga film, by co-sputtering of this target and an elemental Sb target by adjusting the relative power of the two sputter sources to obtain the required film composition. The deposition of relatively thick films enabled us to obtain sufficient material (a few tens of mg) required for NMR spectroscopy. The deposition was conducted at room temperature in an argon atmosphere at a pressure of 0.27 Pa, using a sputtering power of 20 W on the GaSb target for the film with 50 at. % Ga, and 15 W on this target and 20 W on the Sb target for the film with 15 at. % Ga. The film compositions were determined using Rutherford backscattering spectrometry and were found to be slightly Sb rich compared to the nominal compositions (~14 and 46 at. % Ga). These two samples are referred to, in the subsequent discussion, as Ga_{14} and Ga_{46} for the sake of brevity. The as-deposited films were confirmed to be x-ray amorphous and were lifted off for subsequent NMR and x-ray diffraction measurements, by dissolving the PMMA in acetone for 15 min.

X-ray diffraction and absorption data at ambient conditions were collected on the as-deposited amorphous films at beamline 12.2.2 of the Advanced Light Source,[20] using well-focused x-ray beam with a spot size of about 10×10 μm and energies of 30 keV ($\lambda = 0.4133$ Å) and 20 keV ($\lambda = 0.6199$ Å), respectively. The diffraction data were collected to $Q \sim 10$ Å^{-1} at 30 keV. A MAR 345 image plate detector was used to collect diffraction images. The sample-to-detector distance and the detector tilt angles were measured using powder diffraction from a LaB_6 standard. The x-ray beam was 99% horizontally polarized and all geometric and polarization corrections were made during the angular integration using the program FIT2D.[21] Details of the experimental methods and data analysis procedures can be found in our previous publications.[22,23] The ambient densities of the as-deposited amorphous Ga_{14} and Ga_{46} films were measured using combined diffraction and absorption data following the method of Shen *et al.*[24] A 120 μm thick rhenium gasket was indented to a thickness of about ~30 μm using a diamond anvil cell with 400 μm culet diamond. Three 90 μm holes were drilled in the indentation. One was filled with NaCl, which served to determine the gasket thickness experimentally, and the others with samples, Ga_{14} and Ga_{46} (Fig. 1). The contrast of transmitted intensities through these materials was measured and combined with the molar volumes of the NaCl and Re as obtained from their Bragg diffraction patterns to calculate the densities of NaCl and Re. The sample thickness l can then be expressed as

$$l = \ln(I_{NaCl}/I_{\mathrm{Re}})/(\mu_{\mathrm{Re}}\rho_{\mathrm{Re}} - \mu_{NaCl}\rho_{NaCl}),$$

where I_{NaCl} and I_{Re} are transmitted x-ray intensities that were directly measured using a pin diode (Fig. 1) and the mass absorption coefficients μ at studied energies were obtained from the online database of National Institute of Standards and Technology.[25] By assuming the same thickness across the samples and the calibrant, the densities of the samples were obtained using the following relation for each sample:

$$\rho_{sample} = [\ln(I_{NaCl}/I_{sample}) + \mu_{NaCl}\rho_{NaCl}l]/\mu_{sample}.$$

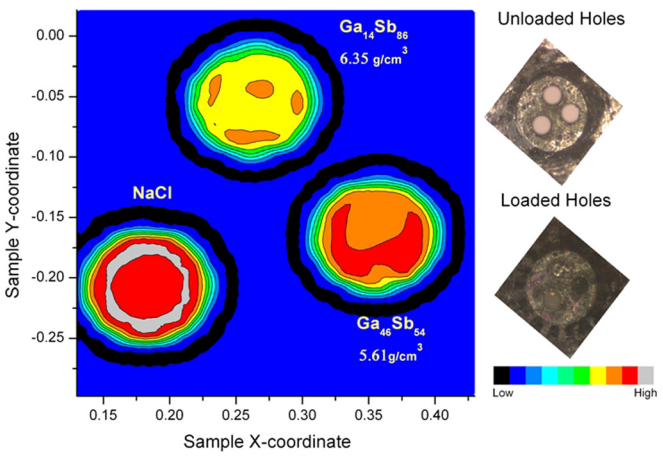

FIG. 1. Triple hole (filled with NaCl and amorphous Ga_{14} and Ga_{46}) configuration of the rhenium gasket between two diamond anvils. X-ray transmission profile was obtained by scanning the sample position in both X and Y directions at steps of 10 μm with x-ray beam size of 10×10 μm. The microscope images were captured before and after sample loading. The color bar at bottom right represents transmission intensities.

Sample thickness and densities of amorphous Ga_{46} and Ga_{14} samples were calculated as $28.8 \pm 1\,\mu m$, $5.61\,g/cm^3$, and $6.35\,g/cm^3$, respectively. The typical errors of $\pm 1.0\,\mu m$ and $\pm(0.05)\,g/cm^3$ in thickness and density measurements, respectively, are estimated from the uncertainties in x-ray transmission intensities of ~0.3% at 20 keV monochromatic x-ray energy and from that in the densities of NaCl and Re calibrants (±3%).

The ^{71}Ga magic-angle-spinning (MAS) NMR spectra of the as-deposited amorphous Ga_{46} film and commercially obtained bulk crystalline GaSb were collected using a Bruker Avance500 spectrometer operating at a magnetic field of 11.7 T (^{71}Ga resonance frequency = 152.5 MHz) using a 2.5 mm Bruker CPMAS probe. Crushed samples were taken in ZrO_2 rotors and were spun at 30 to 34 kHz. Single-pulse spectra were collected using a solids $\pi/10$ pulse (0.15 μs) and a recycle delay of 0.2 s. The ^{71}Ga MAS spectra of the as-deposited amorphous Ga_{14} film and its crystallized product were collected using a Varian spectrometer operating at a magnetic field of 16.4 T (^{71}Ga resonance frequency = 214.1 MHz) using a 2.5 mm MAS probe. Crushed samples were taken in ZrO_2 rotors and were spun at 25 kHz. Spectra were collected using a Hahn-echo pulse sequence with $\pi/2$ and π pulse lengths of 0.6 and 1.2 μs, respectively, and a recycle delay of 0.2 s. 10 k to 65 k scans were averaged and Fourier transformed to obtain each spectrum. All ^{71}Ga spectra were referenced to a 1M solution of $GaNO_3$.

The ^{71}Ga triple-quantum MAS (3QMAS) NMR spectrum of the as-deposited amorphous Ga_{46} film was collected with a Bruker DRX spectrometer at 19.6 T and 25 kHz MAS using a shifted-echo sequence[26] with rotor-synchronized t_1 increments;[27] a total of eight t_1 increments were acquired with ~100 000 transients averaged for each t_1.[26,27] In addition, the Q-shear method was used to expand the F_1 spectral window for the rotor-synchronized 3QMAS spectrum.[28]

The ^{121}Sb NMR spectra were collected with a Bruker DRX spectrometer at 19.6 T using the WURST/QCPMG pulse sequence[29] with 120 μs acquisition windows. A 50 μs WURST-80 pulse[30] with a total sweep frequency of 900 kHz and ~10 kHz *rf* field was used for excitation and refocusing. The transmitter offset was changed by ±600 kHz steps according to the VOCS method[31] for patterns that exceeded the excitation bandwidth of the WURST pulse.

III. RESULTS AND DISCUSSION

The measured density of $5.61\,g/cm^3$ for the amorphous Ga_{46} film is in good agreement with similar densities reported in the literature for amorphous GaSb under ambient conditions ($5.6 \pm 0.1\,g\,cm^{-3}$).[15,16] Although there is no prior report in the literature of the density of amorphous $Ga_{14}Sb_{86}$, the measured density of $6.35\,g/cm^3$ is consistent with and somewhat lower than that reported for amorphous Sb ($6.60\,g/cm^3$).[32] Comparable densities (~$6.1\,g/cm^3$) are also proposed in the literature for amorphous $Ge_{15}Sb_{85}$.[33]

The ^{71}Ga MAS NMR spectrum of the as-deposited, amorphous Ga_{46} film is compared in Fig. 2 with that of the bulk GaSb crystal. The spectrum of the crystal is characterized by a relatively narrow, single resonance with a Gaussian

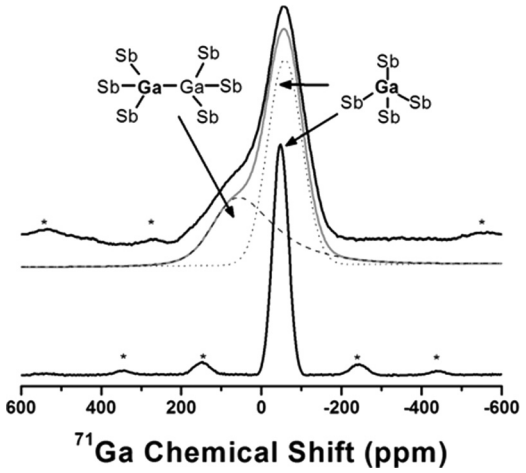

FIG. 2. ^{71}Ga MAS NMR spectra of crystalline GaSb (bottom) and as-deposited amorphous Ga_{46} film (top). Asterisks denote spinning side bands. A two-component simulation of the top spectrum is shown with grey lines. The component denoted by dotted line is a Gaussian line shape while that denoted by the dashed line is a quadrupolar broadened line shape with a Czjezk distribution of C_Q values. Structural cartoons show local Ga coordination environments and their assignments to corresponding ^{71}Ga MAS NMR signals.

line shape centered at ~−50 ppm that corresponds to the Ga atoms in tetrahedral coordination with Sb. The ^{71}Ga MAS NMR spectrum of amorphous Ga_{46}, on the other hand, is characterized by two resonances. The dominant signal centered near −60 ppm can be assigned to a $GaSb_4$ tetrahedral environment as in the bulk crystal, broadened by structural disorder. This is the only signal that is observed in the ^{71}Ga 3QMAS NMR spectrum of the as-deposited amorphous Ga_{46} film, as shown in the 3QMAS projection of this spectrum in Fig. 3. The localization of the intensity of this ^{71}Ga 3QMAS NMR spectrum along the diagonal indicates that the corresponding line width in the MAS spectrum for this site is controlled by chemical shift dispersion from structural disorder and second order quadrupolar broadening is not significant. The ^{71}Ga MAS NMR spectrum of amorphous Ga_{46} also shows a partially resolved shoulder near 100 ppm, broadened by quadrupolar interaction with a distribution of quadrupolar

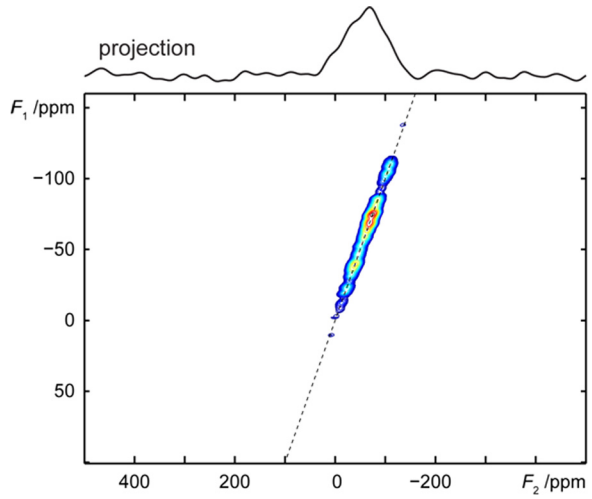

FIG. 3. Contour plot of the ^{71}Ga 3QMAS NMR spectrum of as-deposited Ga_{46} film. The 3QMAS projection is shown on top.

coupling constants C_Q (Fig. 2). The large shift of this resonance to higher frequency, compared to that characteristic of the $GaSb_4$ site is consistent with the presence of Ga-Ga homopolar bonds in the nearest neighbor coordination environment of Ga atoms, presumably corresponding to tetrahedra with one Ga-Ga and three Ga-Sb bonds-forming ethane-like Ga_2Sb_6 environments (Fig. 2) in the amorphous structure. The absence of this resonance in the ^{71}Ga 3QMAS NMR spectrum in Fig. 3 indicates a large quadrupolar broadening for these Ga sites since the 3QMAS efficiency strongly favors sites with small C_Q values. The large C_Q is consistent with the lowering of tetrahedral site symmetry due to the formation of Ga-Ga bonds. Simulation of the MAS spectrum with Gaussian and quadrupolar-broadened line shapes for the two sites (Fig. 2) indicates that ~40% of the Ga atoms exist in such environments in amorphous Ga_{46} with a C_Q of ~9 MHz, and hence the average Ga-Sb coordination number in this material is ~3.6.

It may be noted that the composition of this film is deficient in Ga compared to GaSb stoichiometry and hence the formation of Ga-Ga bonds is rather unexpected. However, this result is consistent with a previous report based on Ga K-edge EXAFS spectroscopy that conjectured the possible formation of Ga-Ga homopolar bonds and reported a Ga-Sb coordination number of ~3.7 in amorphous GaSb.[14,15]

The violation of chemical order in the form of Ga-Ga homopolar bonding implies the formation of an equivalent amount of Sb-Sb bonds in $SbSbGa_3$ tetrahedra in amorphous Ga_{46}. Such Sb environments are expected to have lower site symmetry and hence large quadrupolar broadening compared to the cubic $SbGa_4$ site. The ^{121}Sb WURST/QCPMG NMR spectra of the amorphous Ga_{46} film and of the bulk GaSb crystal are compared in Fig. 4. The spectrum of the GaSb crystal shows a relatively narrow (full width at half maximum of ~0.12 MHz) ^{121}Sb line shape consistent with the cubic site symmetry of the $SbGa_4$ tetrahedral environment in the structure. The ^{121}Sb line shape of amorphous Ga_{46} clearly shows this relatively narrow component corresponding to the $SbGa_4$ tetrahedral environment, superimposed on a broad component with large quadrupolar coupling constant that can indeed be associated with the formation of Sb-Sb bonds in the structure (Fig. 4).

The ^{71}Ga MAS NMR spectrum of the as-deposited amorphous Ga_{14} film is compared in Fig. 5 with that of the crystal phase(s) obtained upon isothermal crystallization of the film at 290 °C for 10 min. The ^{71}Ga MAS NMR line shape of amorphous Ga_{14} is characterized by significant quadrupolar broadening and a large shift to higher frequency (190 ppm) compared to that of the crystallized product which shows a relatively narrow signal characteristic of crystalline GaSb (Fig. 2). Simulation of the ^{71}Ga MAS NMR line shape of amorphous Ga_{14} (Fig. 5), under the assumption that it is solely broadened by quadrupolar coupling, yields a quadrupolar coupling constant $C_Q \sim 12$ MHz associated with the Ga site. This large C_Q, in combination with the large high-frequency shift of this signal compared to those characteristic of tetrahedral Ga environment, indicates that the Ga atoms in amorphous Ga_{14} film are most likely threefold coordinated, presumably forming $Ga\text{-}Sb_3$ pyramids and thus occupying similar sites as Sb atoms that are expected to be present as corner-shared $Sb\text{-}Sb_3$ pyramids as in amorphous Sb. It may be noted here that a recent X-ray absorption spectroscopic study of as-deposited $Ge_{15}Sb_{85}$ films has indicated fourfold coordination environment for the Ge atoms.[33] This difference between Ge and Ga atoms in their coordination numbers in the as-deposited films is not surprising

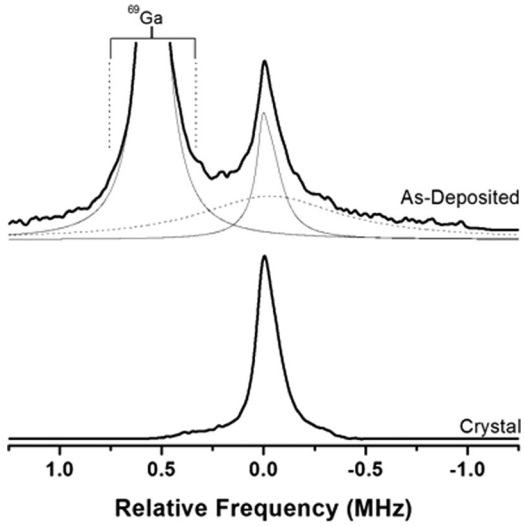

FIG. 4. ^{121}SbWURST/QCPMG NMR spectra of as-deposited Ga_{46} (top) and of crystalline GaSb (bottom), acquired at 19.6 T. The peak at ~0.5 MHz in the top spectrum corresponds to resonance from ^{69}Ga nuclides in the sample. The absence of this ^{69}Ga peak in the bottom spectrum is due to narrower frequency range used for excitation in the case of the GaSb crystal. A three-component simulation of the top spectrum is shown with grey lines. Note the presence of two components for the ^{121}Sb line shape in this spectrum with a narrow component similar to that of the crystal line shape (bottom spectrum) and a broad component (dotted grey line) spanning nearly 2 MHz in frequency range. See text for detailed explanation.

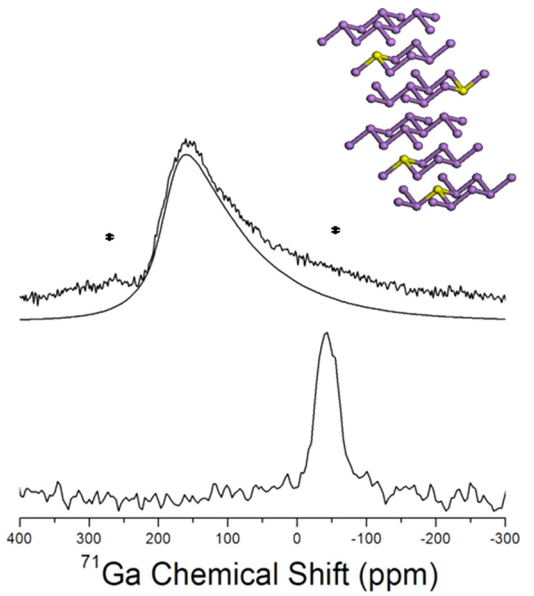

FIG. 5. ^{71}Ga MAS NMR spectra of amorphous (top) and crystallized (bottom) Ga_{14}. Asterisks denote locations of spinning sidebands. Smooth curve immediately below the top spectrum represents a simulation of the spectrum assuming quadrupolar broadening with a Czjezk distribution of C_Q values in the amorphous material. Cartoon in the inset shows schematic local structure in the as-deposited amorphous Ga_{14} phase with threefold coordinated Ga and Sb atoms (Ga and Sb atoms are in yellow and purple, respectively).

considering the fact that the number of valence electrons for these atoms are 4 and 3, respectively. Nevertheless, the threefold coordinated Ga environment in the as-deposited Ga_{14} film is expected to be a metastable structural state indicative of the far-from-equilibrium thermodynamic state of as-deposited amorphous films. The ^{121}Sb wideline WURST/QCPMG NMR spectra of the as-deposited and crystallized Ga_{14} films are shown in Fig. 6. Unfortunately, the full wideline NMR spectrum of the crystallized Ga_{14} film could not be collected due to the poor signal to noise ratio resulting from small sample size (Fig. 6). The similarity between these spectra in terms of their extremely large quadrupolar broadening (line shapes spanning nearly 16 MHz), compared to that in the case of Ga_{46} film, indicates that Sb atoms primarily reside in a lower-symmetry, threefold coordinated environment in both as-deposited and crystallized Ga_{14}. It should be noted here that ^{121}Sb is a relatively large atomic weight nuclide and thus, besides quadrupolar coupling, some part of the line broadening in the ^{121}Sb NMR spectra in Fig. 5 may result from isotropic chemical shift distribution and chemical shift anisotropy. These conclusions regarding threefold coordination of Sb atoms in both as-deposited and crystallized Ga_{14} are in good agreement with similar findings reported in the literature for $Ge_{15}Sb_{85}$ films on the basis of Sb K-edge extended X-ray absorption fine structure (EXAFS) spectroscopy.[33] Therefore, the ^{71}Ga and ^{121}Sb NMR data presented here indicate that the first cycle of crystallization of the as-deposited amorphous Ga_{14} film leads to the formation of crystalline GaSb and Sb phases that must involve significant phase separation via diffusion of Ga atoms and structural reconstruction.

The abovementioned scenarios for the local coordination environments of Ga and Sb atoms in the Ga_{46} and Ga_{14}

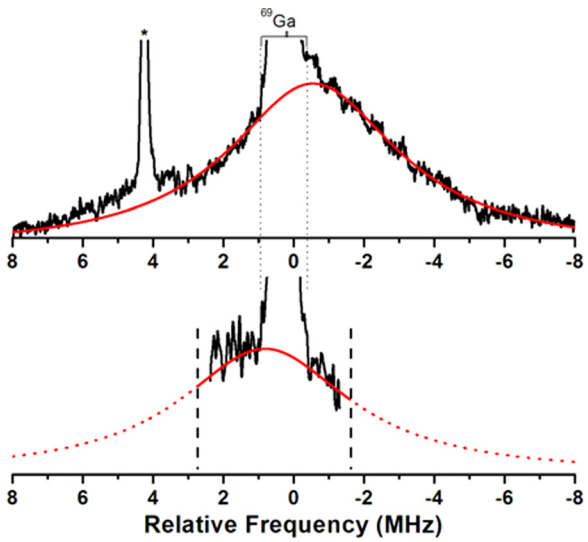

FIG. 6. ^{121}Sb WURST/QCPMG wideline NMR spectra of as-deposited amorphous (top) and crystallized (bottom) Ga_{14} acquired at 19.6 T. The truncated peak near the center of each spectrum corresponds to resonance from ^{69}Ga nuclides in these samples. The sharp truncated peak near 4 MHz in the top spectrum is from probe background. Red line in each spectrum denotes the approximate ^{121}Sb line shape and serves only as a guide to the naked eye. Vertical dashed lines in the bottom spectrum denote the frequency range beyond which NMR data could not be collected within a reasonable period of time due to poor signal to noise ratio resulting from small sample size.

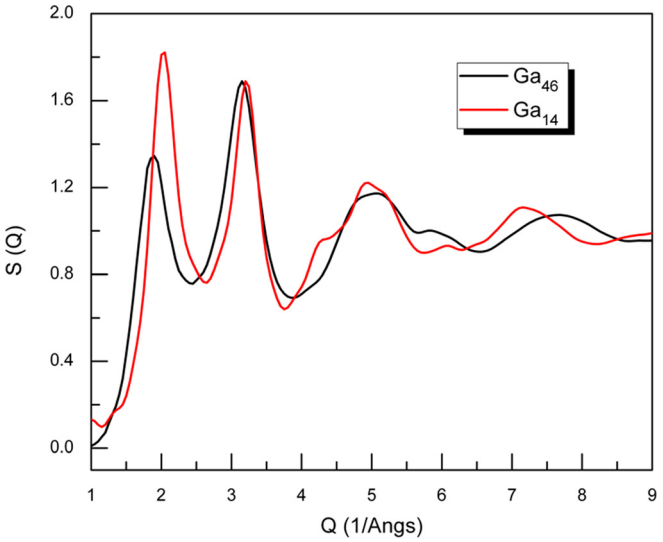

FIG. 7. Experimental x-ray structure factors S(Q) of as-deposited amorphous Ga_{14} (red) and Ga_{46} (black) films.

amorphous films as obtained from ^{71}Ga and ^{121}Sb NMR spectroscopy are corroborated by the average nearest neighbor coordination numbers obtained from x-ray diffraction. The structure factors S(Q) of amorphous Ga_{46} and Ga_{14} are shown in Fig. 7 and the corresponding radial distribution functions (RDFs) G(r) are compared in Fig. 8. Coordination number analysis of the nearest neighbor shell in the RDF of amorphous Ga_{46} yields average Ga-Sb coordination number of ~4.05 and a Ga-Sb distance of ~2.62 Å. The next-nearest neighbor Ga-Ga and Sb-Sb correlation is located near 4.32 Å with a coordination number of ~12. These coordination numbers and bond distances are consistent with the tetrahedral zinc blende structure of crystalline GaSb that is characterized by the Ga-Sb first neighbor and Ga-Ga/Sb-Sb second neighbor coordination numbers of 4 and 12, respectively, and corresponding distances of 2.64 and 4.31 Å, respectively. The strong similarity in the atomic structures at the nearest and next-nearest neighbor levels between amorphous Ga_{46}

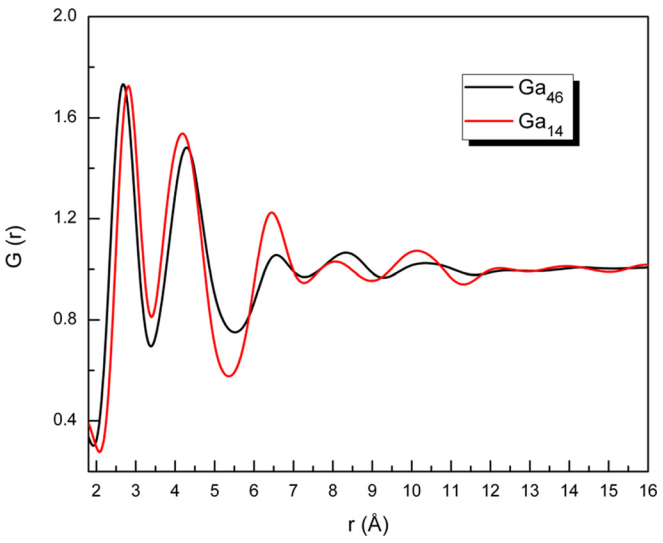

FIG. 8. Radial distribution functions G(r) of as-deposited amorphous Ga_{14} (red) and Ga_{46} (black) films.

and crystalline GaSb is consistent with the fact that the densities of these structures are quite similar (5.6 ± 0.1 g cm^{-3}).[15,16] Similar analyses of the RDF of amorphous Ga_{14} yield average nearest neighbor coordination number of ~2.98 and an average nearest neighbor distance of ~2.84 Å. This average coordination number is consistent with a threefold coordinated Ga environment in amorphous Ga_{14} as indicated by its ^{71}Ga NMR spectrum. The next-nearest neighbor correlation in the RDF of this material is located near 4.23 Å with a coordination number of ~12.8, when integrated out to 5.5 Å. These coordination numbers and bond distances are comparable with the crystal structure of rhombohedral Sb that is characterized by the Sb-Sb first neighbor and second neighbor average coordination numbers of 3 and 12, respectively, and corresponding average distances of 2.70 and 4.19 Å, respectively. It may be noted here that the Sb-Sb second neighbor distances in rhombohedral Sb vary over a large range with two sets of 3 Sb atoms at 3.67 and 4.49 Å and 6 Sb atoms at 4.3 Å.

When taken together, these results elucidate the structural changes accompanying crystallization of as-deposited amorphous Ga_{14} and Ga_{46} films. The structural reconstruction for Ga_{46} must involve bond switching and elimination of Ga-Ga homopolar bonds, and in the case of Ga_{14}, even atomic diffusion, nucleation and growth of GaSb domains. The bond switching is expected to be significantly faster than the nucleation and growth of GaSb nanodomains and is indeed borne out in the switching kinetics of these two as-deposited films. The timescale of the amorphous → crystal phase change for these films was measured using a laser pump-probe setup described in a previous publication.[9] The crystallization kinetics of the as-deposited Ga_{14} film is measured to be significantly slower (~800 ns) compared to that for the as-deposited Ga_{46} film (~60 ns). However, for these phase change materials, after the first cycle of phase change, the amorphous phases obtained by laser remelting show significantly faster kinetics of amorphous → crystal transformation: 5 and 20 ns, respectively, for Ga_{14} and Ga_{46}.[11] This remarkable change in the phase change kinetics upon laser melting clearly indicates that the structures of the melt quenched amorphous Ga_{14} and Ga_{46} may be significantly different from their as-deposited counterparts and possibly more similar to those of the crystalline phases, thereby enabling phase change via a purely displacive mechanism. For example, the Ga-Ga and Sb-Sb homopolar bonding in as-deposited amorphous Ga_{46} and the presence of three-coordinated Ga atoms in as-deposited amorphous Ga_{14} films are likely highly metastable structural moieties attesting to the thermodynamically far-from-equilibrium nature of these films. Such "structural defects" may be removed upon thermodynamic equilibration during melting and the quenched glasses obtained in a memory device after a few phase change cycles would likely be "defect-free" enabling fast phase change kinetics. Indeed, a recent density functional theory based simulation study of as-deposited and melt-quenched GaSb alloy have shown reduction in homopolar bonding and increase in structural similarity with crystalline phase upon melt-quenching.[34] However, the same study indicated a fourfold coordination for Ga atoms in the as-deposited and melt-quenched $GaSb_7$ (12.5% Ga) film. This is in contrast with the experimental results presented here that suggest a threefold coordination environment for Ga in the as-deposited Ga_{14} film. This discrepancy may be related to the preparation method of the starting structures for the DFT simulations of the as-deposited films.

IV. SUMMARY

The short-range structure of as-deposited amorphous Ga_{14} and Ga_{46} alloys and their crystallized products are characterized using ^{71}Ga and ^{121}Sb NMR spectroscopy and synchrotron x-ray diffraction. All constituent atoms are threefold coordinated in Ga_{14} and fourfold coordinated in Ga_{46}, in their as-deposited amorphous states. Significant concentrations of thermodynamically metastable structural moieties are observed in the as-deposited amorphous states of both alloys, including threefold coordinated Ga atoms in Ga_{14} and homopolar Ga-Ga and Sb-Sb bonds in Ga_{46}. Crystallization of the Ga_{46} alloy involves elimination of the homopolar bonds via bond switching and significant structural reconstruction. In contrast, the crystallization of the Ga_{14} alloy results in a change in the Ga coordination number from 3 to 4 and nucleation and growth of crystalline GaSb domains in Sb matrix via phase separation. The crystallization kinetics of the as-deposited amorphous alloys is observed to be nearly an order of magnitude slower than those obtained for the melt-quenched amorphous phases after a phase change cycle of crystallization and melting. This result is indicative of the elimination of the abovementioned thermodynamically metastable structural moieties observed in the as-deposited amorphous phases upon melt quenching, thereby increasing the structural similarity between the amorphous and crystalline states of these alloys and enabling rapid phase change kinetics.

ACKNOWLEDGMENTS

This work was funded by a grant from the National Science Foundation (NSF GOALI 1104869). The National High Magnetic Field Laboratory is supported through the National Science Foundation Cooperative Agreement (DMR-0084173) and by the State of Florida. The Advanced Light Source is supported by the Director, Office of Science, Office of Basic Energy Sciences, of the U.S. Department of Energy (DOE) under Contract No. DEAC02-05CH11231.

[1]D. Lencer, M. Salinga, and M. Wuttig, Adv. Mater. **23**, 2030 (2011).
[2]S. Raoux, W. Welnic, and D. Lelmini, Chem. Rev. **110**, 240 (2010).
[3]S. R. Ovshinsky, Phys. Rev. Lett. **21**, 1450 (1968).
[4]C. M. Lee, W. S. Yen, J. P. Chen, and T. S. Chin, IEEE Trans. Magn. **41**, 1022 (2005).
[5]K. F. Kao, C. M. Lee, M. J. Chen, M. C. Tsai, and T. S. Chin, Adv. Mater. **21**, 1695 (2009).
[6]D. J. Gravesteijn, H. M. van Tongeren, M. Sens, T. Bertens, and C. J. van der Poel, Appl. Opt. **26**, 4772 (1987).
[7]C. C. Chang, K. F. Kao, M.-J. Tsai, T.-R. Yew, and T. S. Chin, J. Nanosci. Nanotechnol. **11**, 10654 (2011).
[8]D. Krebs, S. Raoux, L. Dellman, P. Jonnalagadda, and H. Pozidis, in Materials Research Society—Spring Meeting, San Francisco, USA, 2012.
[9]S. Raoux, A. König, H. Y. Cheng, D. Garbin, R. Cheek, J. L. Jordan-Sweet, and M. Wuttig, Phys. Status Solidi B **249**, 1999 (2012).

[10]Y. Lu, S. Song, Z. Song, and B. Liu, J. Appl. Phys. **109**, 064503 (2011).
[11]H.-Y. Cheng, S. Raoux, and J. Jordan-Sweet, in Proceedings of the 10th European Phase Change and Ovonic Science Symposium (E*PCOS), Zurich, Switzerland, 2011, http://www.epcos.org/library/papers/pdf_2011/Oral-Papers/S5-02.pdf.
[12]A. G. Milnes and A. Y. Polyakov, Solid-State Electron. **36**, 803 (1993).
[13]*Semiconductor Lasers: Fundamentals and Applications*, edited by A. Baranov and E. Tournie (Woodhead Publishing, Cambridge, UK, 2013), 669 p.
[14]A. G. Lyapin, V. V. Brazhkin, S. C. Bayliss, A. V. Sapelkin, J. P. Itié, A. Polian, and S. M. Clark, Phys. Rev. B **54**, R14242 (1996).
[15]A. V. Sapelkin, S. C. Bayliss, A. G. Lyapin, V. V. Brazhkin, and A. J. Dent, Phys. Rev. B **56**, 11531 (1997).
[16]M. Calvo-Dahlborg, U. Dahlborg, O. I. Barkalov, A. I. Kolesnikov, E. G. Ponyatovsky, and A. C. Hannon, J. Non-Cryst. Solids **244**, 250 (1999).
[17]V. K. Fedotov, O. I. Barkalov, E. G. Ponyatovsky, M. Calvo-Dahlborg, U. Dahlborg, and T. Hansen, J. Phys.: Condens. Matter **21**, 045402 (2009).
[18]C.-C. Chang, T.-R. Yew, and T.-S. Chin, Cryst. Eng. Commun. **13**, 5642 (2011).
[19]M. Kaiser, L. van Pieterson, and M. A. Verheijen, J. Appl. Phys. **96**, 3193 (2004).
[20]M. Kunz, A. A. MacDowell, W. A. Caldwell, D. Cambie, R. S. Celestre, E. E. Domning, R. M. Duarte, A. E. Gleason, J. M. Glossinger, N. Kelez *et al*., J. Synchrotron Radiat. **12**, 650 (2005).
[21]A. P. Hammersley, S. O. Svensson, M. Hanfland, A. N. Fitch, and D. Hausermann, in *4th Workshop of the IUCr High Pressure Group on Synchrotron and Neutron Sources, Kek, Japan* (1995), pp. 235–248.
[22]B. Kalkan, S. Sen, and S. M. Clark, J. Chem. Phys. **135**, 124510 (2011).
[23]B. Kalkan, S. Sen, J.-Y. Cho, Y.-C. Joo, and S. M. Clark, Appl. Phys. Lett. **101**, 151906 (2012).
[24]G. Shen, N. Sata, M. Newville, and M. Rivers, Appl. Phys. Lett. **81**, 1411 (2002).
[25]M. J. Berger, J. H. Hubbell, S. M. Seltzer, J. Chang, J. S. Coursey, R. Sukumar, D. S. Zucker, and K. Olsen, *XCOM: Photon Cross Section Database (version 1.5)*, see http://physics.nist.gov/xcom, 2010.
[26]P. J. Grandinetti, J. H. Baltisberger, A. Llor, Y. K. Lee, U. Werner, M. A. Eastman, and A. Pines, J. Magn. Reson., Ser. A **103**, 72 (1993).
[27]D. Massiot, J. Magn. Reson., Ser. A **122**, 240 (1996).
[28]I. Hung, J. Trebosc, G. L. Hoatson, R. L. Vold, J. P. Amoureux, and Z. H. Gan, J. Magn. Reson. **201**, 81 (2009).
[29]L. A. O'Dell and R. W. Schurko, Chem. Phys. Lett. **464**, 97 (2008).
[30]E. Kupce and R. Freeman, J. Magn. Reson., Ser. A **115**, 273 (1995).
[31]D. Massiot, I. Farnan, N. Gautier, D. Trumeau, A. Trokine, and J. P. Coutures, Solid State Nucl. Magn. Reson. **4**, 241 (1995).
[32]F. M. Aymerich and A. Delunas, Phys. Status Solidi A **31**, 165 (1975).
[33]P. Zalden, C. Bichara, J. van Eijk, C. Braun, W. Bensch, and M. Wuttig, J. Appl. Phys. **107**, 104312 (2010).
[34]J. Kalikka, J. Akola, and R. O. Jones, J. Phys.: Condens. Matter **25**, 115801 (2013).